

**Stratal Architecture and Facies Development
in a Middle Wolfcampian Platform Carbonate Reservoir:
University Block 9 Field, Andrews County, Texas**

by
Stephen C. Ruppel
Bureau of Economic Geology
The University of Texas at Austin
University Station, Box X
Austin, TX 78713-8924

ABSTRACT

Cores demonstrate that the Wolfcamp platform carbonate reservoir succession dominantly comprises cycles of basal skeletal wackestones and packstones overlain by skeletal to ooid-rich, grain-dominated packstones. Grikes and other karst-related diagenetic features are common below cycle tops. However, neither facies nor cycles nor diagenesis can be defined by conventional wireline logs. Image logs, when properly calibrated to core, are capable of resolving facies, cycle boundaries, and karst diagenesis, thereby providing the basis for establishing a fieldwide reservoir framework.

INTRODUCTION

Reservoirs developed in platform carbonates of the Wolfcamp Series (lower Permian) have accounted for a small but significant volume of oil production from the Permian Basin. The largest 40 of these reservoirs (those having greater than 1 million barrels of cumulative production) had produced more than 268 million barrels by the end of 1998 (S. P. Dutton, personal communication, 2000). Most of these reservoirs are developed on the northeast side of the Central Basin Platform (Fig. 1).

Because they are commonly associated with more prolific underlying and overlying reservoirs, Wolfcamp reservoirs have been overlooked in terms of detailed study. Until recently, relatively little had been published regarding the depositional and diagenetic controls of reservoir development in these rocks. Studies by Mazzullo and Reid (1989) and Candelaria and others (1992) document the large-scale features of Wolfcamp stratigraphy and facies in the northern Midland Basin and along the east margin of the Central Basin Platform, respectively. Saller and others (1994; Dickson and Saller, 1995; Saller and others 1999 a, b) conducted detailed studies of

Wolfcampian and Pennsylvanian carbonate successions in the Andrews field area in central Andrews County using extensive core control. Their study, which developed models for the cyclicity, diagenesis, and causes of porosity development in Wolfcamp reservoirs, provides critical new information that can serve as an important reference for studies of other Wolfcamp reservoirs. The Wolfcamp reservoir succession at University Block 9 field, a few miles southwest of the Andrews field area, offers a good testing ground for these models.

The purpose of the current study of the University Block 9 Wolfcamp reservoir was to interpret and integrate available core and wireline data to develop a detailed architectural framework for the reservoir that can be used as a basis for distributing petrophysical properties throughout the reservoir and calculating original and remaining resources. As is the case in many carbonate reservoirs, conventional wireline logs provide insufficient control for detailed correlations of facies and cyclicity. An important component of this study was the evaluation of borehole image logs in defining facies, cyclicity, and rock fabrics. This report outlines the results of that study. A core and image-log pair will be on display at the core workshop to illustrate important aspects of the Wolfcamp succession in the field.

SETTING

The University Block 9 Wolfcamp field is one of several Wolfcamp shallow-water platform carbonate reservoirs located along the east side the of the Central Basin Platform (Fig. 1). The field, which was discovered in 1953, is developed on a domal structure (Fig. 2) and is also productive from Devonian Thirtyone limestones and Pennsylvanian Canyon and Cisco limestones. The Wolfcamp reservoir averages 80 ft in thickness at a depth of about 8,400 to 8,500 ft. At present, the field is being operated by Cross Timbers Oil Company.

After producing on primary production throughout the 1950's, the field was unitized in 1960, and a peripheral, miscible gas/water injection flood was begun. Cumulative primary production to this time was 5.5 million barrels (Cone, 1970). Gas/water injection continued until 1970; water injection, still primarily from peripheral wells, continues today. Cumulative production from the reservoir is nearly 28 million barrels. Original oil in place (OOIP) was previously estimated to be about 51 million barrels (Cone, 1970), implying a current recovery efficiency of about 55 percent. Recent study by the Bureau of Economic Geology suggests that OOIP was actually nearly 81 million barrels, indicating a recovery efficiency of 35 percent and almost 22 million barrels of remaining mobile oil in the reservoir.

METHODS

Descriptions of facies, diagenesis, and cyclicity are based on nearly 560 ft of core from six wells in the field (Fig. 2). Thin sections were obtained from each core to refine facies descriptions and characterize rock fabrics. Core-based descriptions were supplemented by image logs (Schlumberger FMI logs), which were available for eight wells (Fig. 2). Image-log response was calibrated to core in one well (Cross Timbers

BA No. 7) in which both core and image logs were obtained. Core-analysis data were available from four wells for porosity and permeability measurement.

REGIONAL STRATIGRAPHY

Several previous workers have argued for the presence of a major unconformity in the middle of the Wolfcamp section in the Permian Basin. For the most part, this unconformity, called the *mid-Wolfcamp unconformity* by many, has been postulated on the basis of studies of fusulinid faunas (Wilde, 1990). Candelaria and others (1992) integrated cores and seismic data with fusulinid biostratigraphy to define and map this apparent hiatus along the east margin of the Central Basin Platform in Ector County. They suggested that the middle Wolfcamp was truncated below this major sequence boundary and that the lower Wolfcamp was overlain directly by the upper Wolfcamp in the platform interior to the west. Work by Saller and others (1999a, b) showed, however, that the middle Wolfcamp is present in central Andrews County farther north along the Central Basin Platform. By comparison, preliminary sequence stratigraphic work by Fitchen and others (1995) in the Sierra Diablo and by Simo and others (2000) in the Hueco Mountains reveals no evidence of a major sea-level fall during the middle Wolfcampian. In the Sierra Diablo there is, however, strong evidence of major truncation and erosion of the Wolfcamp section at the base of the Leonard (Fitchen and others, 1995; Kerans, and others, 2000). Strong evidence of this unconformity in the subsurface appears to be lacking.

Although the question of a middle Wolfcamp hiatus is unsettled, subsurface data (wireline logs and seismic) do support a major sea-level rise accompanied by major backstepping of the platform and subsequent downlap at about the boundary between the middle and upper Wolfcamp. This backstepping, which was documented by Candelaria and others (1992) and also described by Saller and others (1994) in the Andrews field area, is apparent on 3-D seismic data from University Block 9 field (Fig. 3). The actual position of the boundary between the middle and upper Wolfcamp is uncertain. However, biostratigraphic data collected by Saller and others (1999a) suggest that these Wolfcamp reservoirs are entirely middle Wolfcampian (Fig. 3).

STRATIGRAPHY AND FACIES

Correlation and subdivision of the Wolfcamp succession are difficult using wireline logs alone. The irregular presence of shale and uranium-bearing carbonate makes interpretation of the gamma ray problematical. Three gamma-ray log markers can be reasonably well correlated (Figs. 4, 5). The A marker defines the top of the reservoir interval and separates in situ, shallow-water, carbonate platform deposits of the reservoir from overlying allochthonous, interbedded, clastic and carbonate debris-flow deposits of the Upper Wolfcamp. The B marker, which appears to define a major cycle boundary marked by shale- and/or uranium-bearing carbonate, subdivides the reservoir into lower and upper parts. The C marker (Fig. 4) defines the base of the reservoir. For the most part, further subdivision of the reservoir succession with conventional logs is not possible.

The Wolfcamp reservoir succession in University Block 9 field is predominately limestone with subordinate shale and dolostone. Nine basic facies can be recognized from study of the cores from the field. The most common of these are well displayed in core from the Shell 9A No. 1 (Cross Timbers 11SA No. 1) well (Fig. 4); two facies (black shale and dolomitized mudstone-wackestone) are found in only one core each (Fig. 5). Two facies predominate throughout the reservoir: the skeletal buildup facies and the skeletal, grain-dominated packstone facies.

Skeletal Buildup Facies

Skeletal buildup facies consist of skeletal-rich wackestones and packstones that locally grade into boundstones. These are most common in the lower part of the Wolfcamp reservoir succession (Figs. 4, 5). Dominant allochems are tubular forams, phylloid algae, fusulinids, and peloids; crinoids and brachiopods are less common. Bedding is poorly developed, but stylolites are common (Fig. 6A). The skeletal buildup facies appears to be developed as a relatively continuous blanket, about 15 to 20 ft in thickness, across the field (Fig. 5). However, lithology varies significantly between cored wells. In some cores the rocks are mud-rich wackestones, and in others packstones are dominant. Evidence of actual binding by algae into boundstones is rare, as are indications of wave reworking or transport. These rocks probably represent largely in situ organic-rich deposits that accumulated in a low-energy setting. Porosity in these rocks is primarily associated with moldic pores created by dissolution of skeletal allochems; intercrystalline and fracture pores are less common. Porosity and permeability average about 5 percent and 0.37 md, respectively. Although this facies contains a high percentage of the total reservoir pore volume, these rocks typically exhibit lower permeability than packstones and grain-dominated packstones.

Skeletal Grain-Dominated Packstone

Skeletal grain-dominated packstone and packstones together constitute the most abundant facies in the Wolfcamp succession. These rocks, which form cycle tops in both the lower and upper parts of the Wolfcamp (Figs. 4, 5), typically contain a mixed assemblage of skeletal allochems, including primarily crinoids, fusulinids, forams, and brachiopods. Locally ooids are abundant. In contrast to other Wolfcamp carbonate facies, these deposits are well sorted, indicating current reworking. Texture, sorting, and position at cycle tops suggest that these deposits accumulated in relatively high energy, shallow-water conditions. Porosity and permeability average about 8 per cent and .48 md, respectively; intercrystalline and moldic pores are dominant. Locally where intercrystalline pores are abundant, porosity exceeds 19 percent, with permeabilities of more than 30 md.

In some wells, this facies is crosscut by subvertical, sediment-filled grikes (Fig. 7A). These features were probably formed during exposure and dissolution associated with sea-level fall at cycle boundaries. Grikes are filled with friable silt and clay presumably derived from clastics deposited during sea-level lowstand.

Nodular Skeletal Wackestone-Packstone

The nodular, skeletal, wackestone-packstone facies is composed of a mixed assemblage of fine-grained skeletal debris. Stylolites and nodular bedding are common throughout (Fig. 8A). These rocks are closely associated with the skeletal, grain-dominated, packstone facies in the middle and upper parts of the facies succession. In many cores they cyclically alternate with the grain-dominated facies, forming cycle bases (Fig. 5). The mud-rich texture of these rocks, coupled with the presence of nodular bedding, suggests that they were deposited in low-energy conditions. Porosity and permeability average about 3 to 4 percent and 0.5 md, respectively.

Fusulinid Wackestone-Packstone

Fusulinid wackestone-packstones are most common at cycle bases in the upper part of the reservoir above the B marker (Fig. 3). They contain abundant fusulinids, along with lesser quantities of forams and other skeletal allochems. On the basis of other studies of Permian platform successions (Sonnenfeld, 1991; Kerans and Fitchen, 1995), these deposits probably represent the deepest water conditions in the Wolfcamp platform succession. Porosity and permeability are generally quite low, with porosity averaging 1 to 2 percent and permeability less than 0.1 md.

Oncolitic Algal Wackestone

The oncolitic algal wackestone facies is restricted to the upper part of the reservoir, above the B marker (Figs. 4, 5). Oncolites, the principal components of these rocks, are irregularly coated grains that average 0.5 to 3 cm in diameter. Like those described by Saller and others (1994), oncolites appear to be coated by tubular foraminifera and *Tubiphytes*. These deposits also contain a mixed assemblage of skeletal allochems, including crinoids, brachiopods, fusulinids, and mollusks. Studies of other Permian successions in the Permian Basin (Ariza, 1998; Ruppel and others, 2000) demonstrate that oncolites are associated with transgressive deposits above sequence boundaries. Porosity and permeability in these rocks are low.

Shale

Where recovered in core, the shale facies is composed of black, unfossiliferous, fissile shale. In the Wolfcamp reservoir succession, shale is essentially restricted to the base of the B marker (Fig. 5). Logs indicate other shale intervals below and above the reservoir. However, conventional gamma-ray logs are misleading regarding shale extent. Although the positive gamma-ray deflection that is associated with shale at the base of the B marker in the Cross Timbers BA No. 7 well (Fig. 5) is continuous across the field, spectral gamma-ray logs and borehole image logs reveal that shale is much more limited in extent (Fig. 5). Positive gamma-ray deflections in many other wells are associated with uranium-rich transgressive carbonate rather than shale (Fig. 5). Judging from core and image-log data, shale appears to be most common in areas where the underlying cycle-top skeletal packstone facies has been karsted. A similar relationship was observed in the Pennsylvanian section at University Block 9 field (R. Barnaby, personal communication, 1999) and in the Andrews field area (Saller and others, 1999a). The irregular distribution of shale at the base of the B

marker is probably the result of local infilling of topographic lows by clay muds during marine flooding of the platform during sea-level rise.

Other Minor Facies

Three facies are only locally expressed in cored wells. Peloid mudstone-wackestone is encountered in several cores as thin, cycle-base deposits. Peloid packstone is present in only a single core low in the reservoir section (Fig. 5). Both facies, which are composed of fecal pellets and fine-grained skeletal debris, represent restricted, relatively low energy depositional conditions. Neither appears to contribute to reservoir performance. Dolomitized mudstone-wackestone was observed in only one core (Fig. 5). Original depositional texture is obscured by dolomitization but is likely to have been mud dominated. Intercrystalline porosity ranges to 8 percent (average, 0.46); permeability ranges to 0.5 md (average, 0.01 md).

CYCLE AND SEQUENCE STRATIGRAPHY

Facies-stacking patterns in cored wells indicate two possible scales of cyclicity. In several of the cored wells, high-frequency cycles are well expressed in the middle of the reservoir section below the B marker as alternations between cycle-base nodular, skeletal wackestone-packstones and cycle-top packstones and grain-dominated packstones (Figs. 4, 5). These cycles average 10 to 15 ft in thickness. Similar cycles above the B marker are somewhat thicker and typically consist of basal fusulinid wackestone or oncolitic, algal wackestone and capping skeletal grain-dominated packstone. Cyclicity is poorly developed in the skeletal buildup facies at the bottom of the reservoir interval. Overall, eight or nine cycles can be defined from existing cores in the University Block 9 Wolfcamp reservoir. This agrees well with the eight cycles defined by Dickson and Saller (1995) in Andrews field.

Facies-stacking and distribution patterns suggest that the B marker defines a longer term cycle boundary. The evidence is threefold. First, karsting and dissolution immediately below the B marker suggest exposure and meteoric diagenesis during sea-level fall or lowstand. Dickson and Saller (1995) also interpreted this surface to have undergone subaerial exposure and diagenesis in the Andrews field area. Second, the local mantling of the B marker surface by transgressive shales suggests the development of an erosional/diagenetic topography associated with sea-level fall. Third, fusulinid-rich rocks, which are essentially absent below the B marker, are abundant above it (Fig. 5). Their appearance defines a substantial facies offset representing a significant rise in relative sea level above this boundary.

It is tempting to conclude that the B marker represents the boundary between the middle and upper Wolfcamp. Cores and image logs document deep-water debris flows above the reservoir succession, suggesting a continued upward deepening. However, Saller and others (1999a) reported that the entire Wolfcamp reservoir succession at Andrews field is middle Wolfcampian. It thus appears that the sea-level rise event documented above the B marker represents a sequence boundary within the middle Wolfcamp and that the middle/upper Wolfcamp boundary lies above the reservoir.

A critical test of whether or not cycles defined from 1-D data sets (cores or logs) are truly the result of sea-level rise/fall is their continuity. Because conventional logs are insensitive to most cycle boundaries in the Wolfcamp (other than the probable sequence boundary at B), correlation and testing of cycle continuity are not possible with these logs. Comparison of closely spaced cores suggests that some of these cycles do extend over parts of the field, but their full continuity is not clear.

IMPROVED RESOLUTION OF FACIES AND STRATIGRAPHY FROM IMAGE LOGS

Although core coverage in the field is adequate for general identification of facies and cyclicity, it is insufficient for characterization of the geological architecture of the Wolfcamp reservoir. None of the conventional logs provides required resolution of cycles and facies needed for detailed correlation and mapping of reservoir units. However, eight borehole image logs of the reservoir have proven especially valuable in integrating core and conventional wireline log data into a detailed geological model (Fig. 2).

Critical to the effective use of borehole image logs is the proper calibration of images to core features. About 50 ft of core was obtained in the BA No. 7 well (Fig. 9), along with an image log (Schlumberger FMI log) over the complete Wolfcamp section. On the basis of comparisons of image log and core, three depositional facies and one diagenetic facies can be identified from image logs. One of the major productive facies in the reservoir, the skeletal buildup facies, is characterized on the image log by a spongelike appearance (Fig. 6b). Cycle-top, skeletal, grain-dominated packstones, the second-most-important reservoir facies, have a granular or homogenous image-log appearance (Fig. 7b). Mud-rich, cycle base, nodular, skeletal wackestone-packstones appear similar to the skeletal buildup facies, having irregular laminations and a spongelike matrix appearance (Fig. 8b). Transgressive fusulinid wackestone-packstones can also be identified on image logs.

In addition to depositional facies, both diagenetic features and cycle boundaries can be defined from image logs. Overprinting karst diagenesis, which has chiefly affected cycle-top, skeletal, grain-dominated packstones, is readily identified by the image logs (Fig. 6b). Because the major facies types can be defined, facies-stacking patterns can be determined, thus leading to the definition of cycle boundaries. Figure 10a illustrates a typical cycle boundary between karsted, skeletal, grain-dominated packstone and overlying nodular, skeletal wackestone-packstone. Note that the image log resolves the two facies, the contact between them, and the dissolution pit below the cycle top.

Once the image log is calibrated to core, it is possible to assign facies and identify cycle boundaries throughout the reservoir. Examination of image-log character across the entire field indicates that three depositional facies can be confidently identified: skeletal/peloidal packstone, fusulinid wackestone-packstone, and stylolitic, nodular wackestone-buildup (Fig. 11). The first two of these correspond directly to the skeletal/peloidal, grain-dominated packstone and fusulinid wackestone-packstone core facies, respectively. The stylolitic, nodular, wackestone-buildup image-log facies includes both the nodular, wackestone-packstone facies and skeletal buildup facies

because these two core facies cannot be rigorously separated on the image log. The distribution of karst-overprinting diagenesis can also be defined from the image logs (Fig. 11).

A comparison of Wolfcamp facies and cyclicity defined from core (Fig. 9) with that defined from image-log data (Fig. 11) demonstrates the value of image logs in geological characterization. Essentially all of the major facies, both depositional and diagenetic, are identified with the image log. In addition, because of its longer vertical coverage, more of the reservoir extent can be identified than with typically shorter cores. Interpretation of the image log suggests that the Wolfcamp reservoir section comprises parts of five cycles, each of which averages about 25 ft in thickness (Fig. 11). This interpretation differs from that derived from examination of the core alone. Thinner cycles tentatively identified from core are not recognizable on the image log and thus may be due to local variations in depositional conditions rather sea level rise and fall events.

By integrating cores and Image logs throughout the field it is possible to establish a cycle-based framework for the Wolfcamp reservoir at University Block 9 field (Fig. 12). This framework is based on image-log correlations of primary facies and cycle boundaries and represents a far more accurate picture of the distribution of major rock fabric elements in the reservoir than could be obtained from cores and conventional logs alone. Particularly noteworthy is the resolution of facies changes between skeletal/peloidal packstone and stylolitic, nodular, wackestone-buildup facies in the upper (A-B) and lower (B-C) parts of the reservoir (Fig. 12). Because of the contrasting pore types developed in each of these facies, delineation of facies changes is especially important to accurate permeability modeling.

CORE ON DISPLAY

Core from the BA No. 7 well (Fig. 2) illustrates the major facies in the Wolfcamp at University Block 9 field (Fig. 9). The facies succession here is similar to that seen in other cores throughout the field but differs from others in three important respects: (1) more abundant karst solution features (grikes), (2) lower porosity, and (3) the presence of a thick shale interval above the B marker. It is possible that the three are related. The abundance of grikes suggests that this area of the field has undergone more extensive karst diagenesis. Low porosity is the result of infilling of these solution features by clastic sediment introduced during subsequent sea-level lowstand and exposure and perhaps cementation and pore-filling associated with meteoric diagenesis at the same time. A thick shale section may be a signature of enhanced karst diagenesis and porosity reduction. Shales appear to be most common above low-porosity sections and absent over porous Wolfcamp carbonates (Fig. 12).

The image log from BA No. 7 well (Fig. 11) illustrates the key image-log characteristics of major Wolfcamp facies in the reservoir. Both core and image logs will be available at the workshop for examination and comparison.

SUMMARY

Examination of cores and wireline image-logs indicates that the Wolfcamp platform carbonate reservoir succession in University Block 9 field comprises 5 depositional cycles and as many as nine facies. Reservoir porosity and permeability are concentrated in cycle top grain-dominated packstones and cycle-base skeletal wackestones/buildups. Although cores provide maximum detail in characterization of facies, image-logs are superior in the definition of facies continuity and cyclicity. Image-logs define four major depositional facies that exist throughout the field, including both reservoir facies, and permit the identification and correlation of cycle boundaries. They also identify areas of cycle-top karst diagenesis, which appears to play a role in porosity variations in the reservoir. When calibrated to cores, image-logs are an extremely valuable subsurface tool in characterizing important details of carbonate facies distribution and cyclicity that are key to developing an accurate reservoir model..

ACKNOWLEDGMENTS

Discussions with Roger Barnaby regarding interpretations of architecture and facies development and diagenesis in the underlying Pennsylvanian at University Block 9 field were helpful in gaining an understanding of the Wolfcamp section. Thanks to Jeff Heyer, Magell Candelaria, Steve Weiner, Bob Sunde, and Art Wuensche of Cross Timbers Oil Company for providing data for the study and important information on the reservoir history. Jubal Grubb provided critical support in handling and interpreting wireline log data and making correlations. Art Saller freely shared data on the Andrews field area study for purposes of comparison.

Illustrations were prepared under the supervision of Joel L. Lardon, Graphics Manager. The paper was edited by Lana Dieterich. Publication is authorized by the Director, Bureau of Economic Geology.

REFERENCES

- Ariza, E. E., 1998, High-resolution sequence stratigraphy of the Leonardian lower Clear Fork in the Permian Basin, West Texas: ≈ The University of Texas at Austin, Master's thesis, 128 p.
- Candelaria, M. P., Sarg, J. F., and Wilde, G. L., 1992, Wolfcamp sequence stratigraphy of the eastern Central Basin Platform, *in* Mruk, D. H., and Curran, C., eds., Permian Basin exploration and production strategies: application of sequence stratigraphic and reservoir characterization concepts: West Texas Geological Society Publication 92-91, p. 27–44.
- Cone, C., 1970, The case history the University Block 9 (Wolfcamp) field—A gas-water injection secondary recovery project: Society of Petroleum Engineers, Paper SPE 2837.

- Dickson, J. A. D., and Saller, A. H., 1995, Identification of subaerial exposure surfaces and porosity preservation in Pennsylvanian and lower Permian shelf limestones, eastern Central Basin Platform Texas, *in* Budd, D. A., Saller, A. H., and Harris, P. M., eds., *Unconformities in carbonate shelf strata — their recognition and the significance of associated porosity: AAPG Memoir 57*, p. 239–257.
- Fitchen, W. M., Starcher, M. A., Buffler, R. T., and Wilde, G. L., 1995, Sequence stratigraphic framework and facies models of the early Permian platform margins, Sierra Diablo, West Texas, *in* Garber, R. A. and Lindsay, R. F., eds., *Wolfcampian-Leonardian shelf margin facies of the Sierra Diablo—seismic scale models for subsurface exploration: West Texas Geological Society Publication 95-97*, p. 23–66.
- Kerans, Charles, and Fitchen, W. M., 1995, Sequence hierarchy and facies architecture of a carbonate ramp system: San Andres Formation of Algerita Escarpment and Western Guadalupe Mountains, West Texas and New Mexico: The University of Texas at Austin, Bureau of Economic Geology Report of Investigations No. 235, 86 p.
- Kerans, C., Kempter, K., Rush, J., and Fisher, W. L., 2000, Facies and stratigraphic controls on a coastal paleokarst, Lower Permian Apache Canyon, *in* Lindsay, R., Trentham, R., Ward, R. F., and Smith A. H., eds., *Classic Permian geology of West Texas and southeastern New Mexico, 75 years of Permian Basin oil and gas exploration and development: West Texas Geological Society Publication 00-108*, p 55–82.
- Mazzullo, S. J., and Reid, A. M., 1989, Lower Permian platform and basin depositional systems, northern Midland Basin, Texas, *in* Crevello, P. D., Wilson, J. L., Sarg, J. F., and Read, J. F., eds., *Controls, on carbonate platform and basin development: SEPM Special Publication 44*, p. 305–320.
- Ruppel, S. C., Ward, W. B., Ariza, E. E. and Jennings, J. W. , Jr., 2000, Cycle and sequence stratigraphy of Clear Fork reservoir-equivalent outcrops: Victorio Peak Formation, Sierra Diablo, Texas, *in* Lindsay, R., Trentham, R., Ward, R. F., and Smith A. H., eds., *Classic Permian geology of West Texas and Southeastern New Mexico, 75 years of Permian Basin oil and gas exploration and development: West Texas Geological Society Publication 00-108*, p 109–130.
- Saller, A. H., Dickson, J. A. D., and Boyd, S. A., 1994, Cycle stratigraphy and porosity in Pennsylvanian and lower Permian shelf limestones, eastern Central Basin Platform, Texas: *AAPG Bulletin*, v. 78, no. 12, p. 1820–1842.

- Saller, A. H., Dickson, J. A. D., and Matsuda, F., 1999b, Evolution and distribution of porosity associated with subaerial exposure in upper Paleozoic platform limestones, West Texas: AAPG Bulletin v. 83, no. 11, p. 1835–1854.
- Saller, A. H., Dickson, J. A. D., Rasbury, E. T., and Ebato, T., 1999a, Effects of long-term accommodation changes on short term cycles: Upper Paleozoic platform limestones, West Texas, *in* Advances in carbonate sequence stratigraphy: application to reservoirs, outcrops, and models: SEPM Special Publication No. 63, P. 227–246.
- Simo, J. A., Wahlman, G. P., Beall, J. L., and Stoklosa, M. L., 2000, Lower Permian (Wolfcampian) in the Hueco Mountains: stratigraphic and age relationships, *in* DeMis, W. D., Nelis, M. K., and Trentham, R. C., eds., The Permian Basin: proving ground for tomorrow's technologies: West Texas Geological Publication 00-109, p. 41–50.
- Sonnenfeld, M. D., 1991, High-frequency cyclicity within shelf-margin and slope strata of the upper San Andres sequence, Last Chance Canyon, *in* Meader-Roberts, Sally, Candelaria, M. P., and Moore, G. E., eds., Sequence stratigraphy, facies and reservoir geometries of the San Andres, Grayburg, and Queen Formations, Guadalupe Mountains, New Mexico and Texas: Permian Basin Section, Society of Economic Paleontologists and Mineralogists Publication 91-32, p. 11–51.
- Wilde, G. L., 1990, Practical fusulinid zonation: the species concept; with Permian Basin emphasis: West Texas Geological Society Bulletin, v. 29, no. 7, p. 5–34.

FIGURES

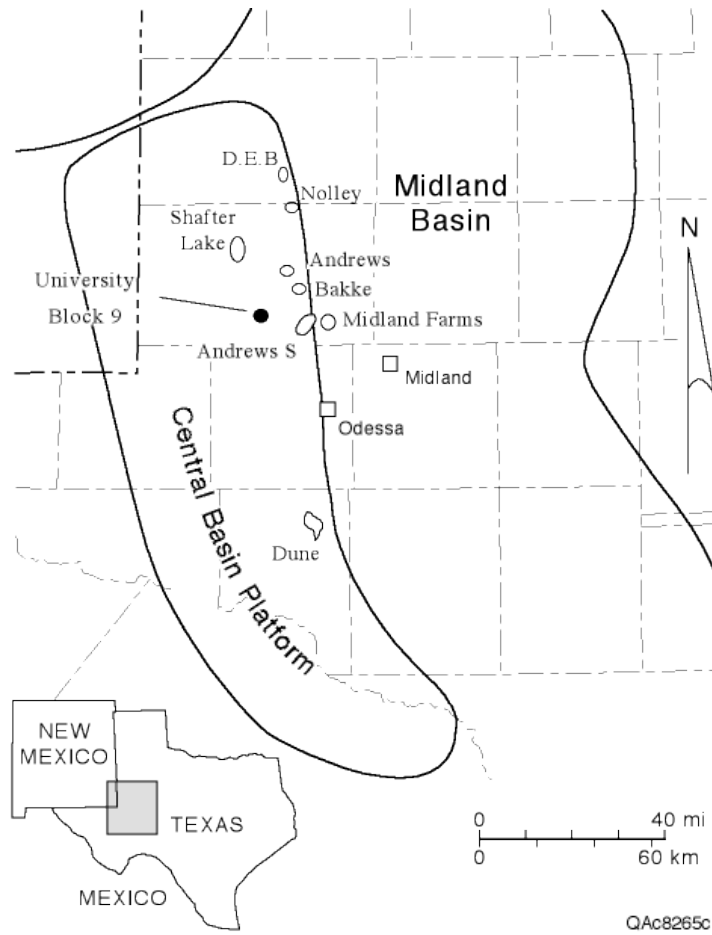


Figure 1. Map of West Texas showing the distribution of large (>10 million barrels cumulative production) Wolfcamp platform carbonate reservoirs in the Permian basin. Outlines of platforms and basins reflect approximate Leonardian paleotopography.

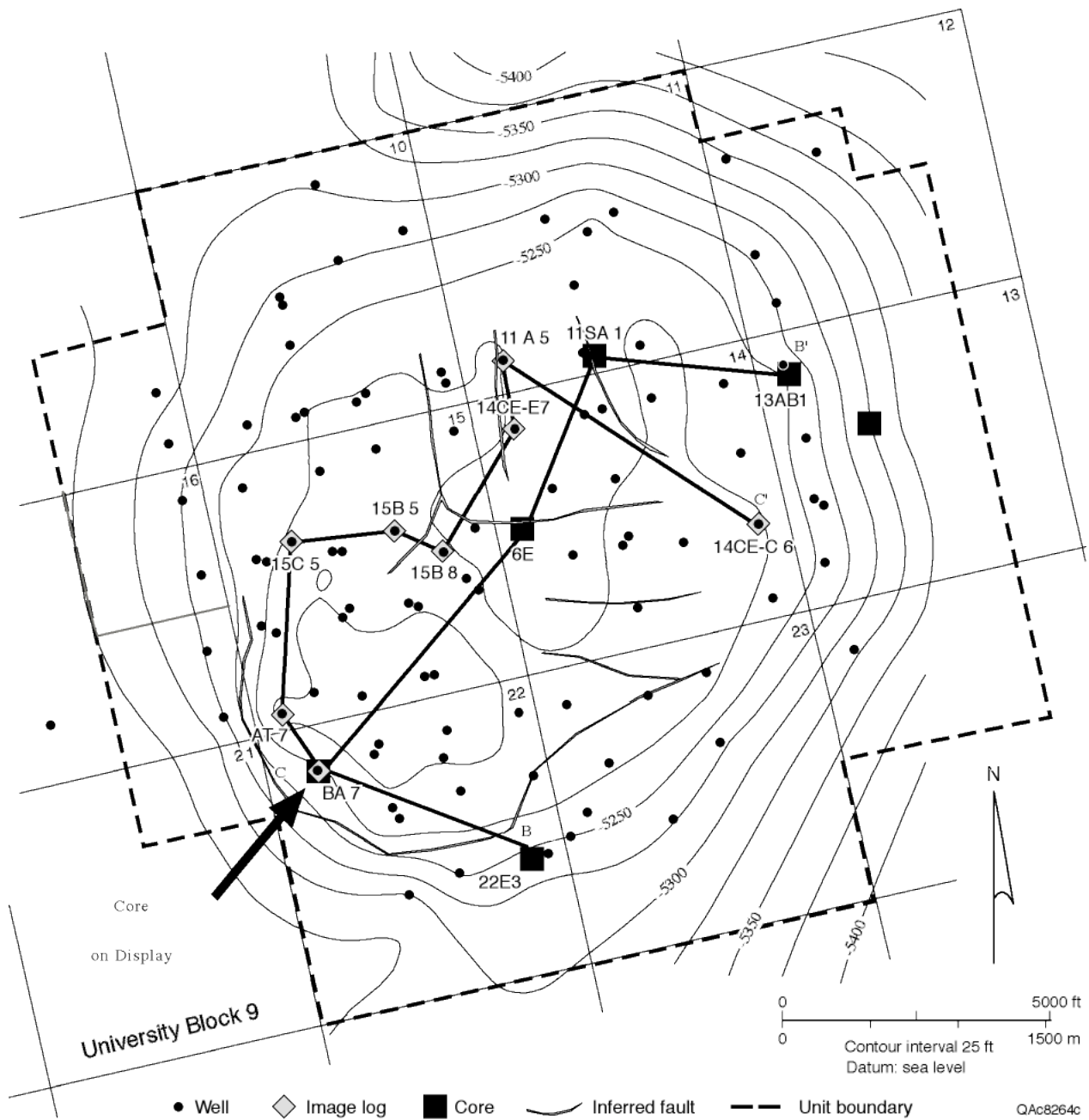


Figure 2. Map of University Block 9 Wolfcamp field showing structure of the Wolfcamp reservoir and the distribution of cores and image logs.

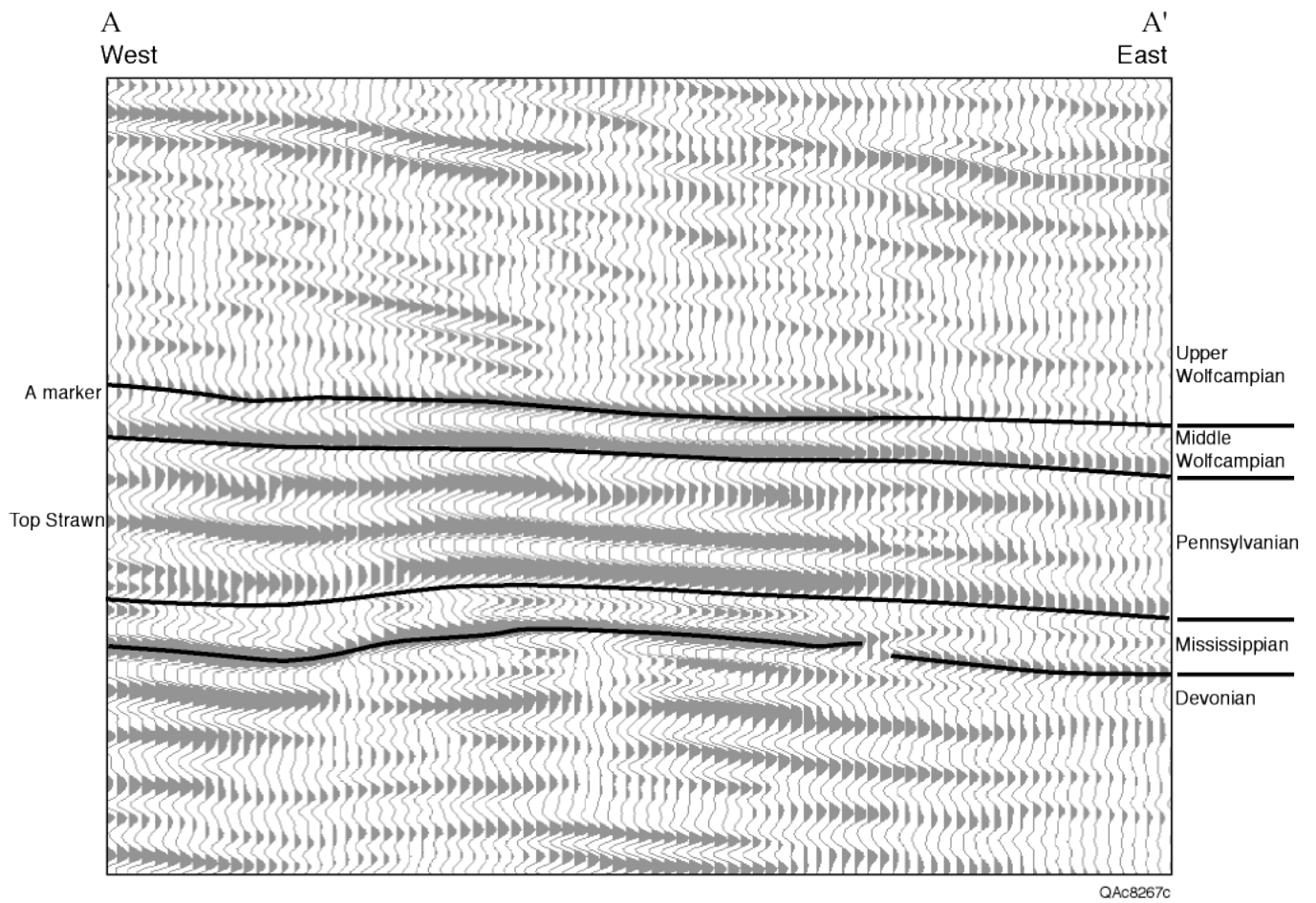
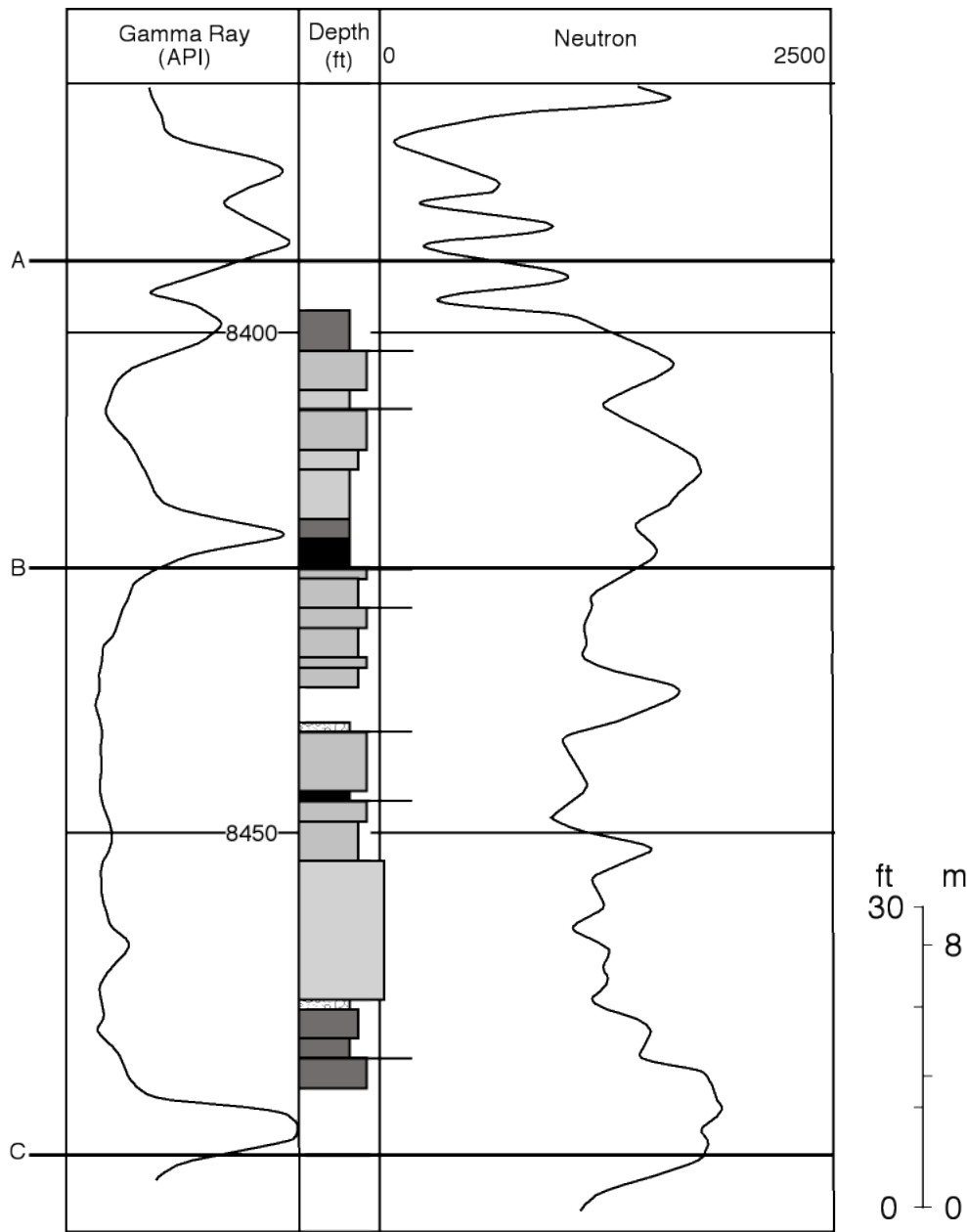


Figure 3. Cross section (A–A') of 3-D seismic volume showing general stratigraphy in the area of University Block 9 field based on core descriptions.



- | | | |
|--|---|---|
|  Well-sorted, grain-dominated skeletal facies |  Oncolitic, algal wackestone |  Grain-dominated packestone |
|  Nodular, mixed skeletal wackestone-packstone |  Peloidal grain-rich packstone |  Packestone Wackestone |
|  Fusulinid wackestone-packstone |  Peloidal mudstone-wackestone | Cycle boundary |
|  Mud-rich to grain-rich algal buildup | | Marker |

Figure 4. Typical vertical Wolfcamp facies succession based on core. University Block 9 field. Shell 9A No. 1(Cross Timbers 11 SA No. 1) well.

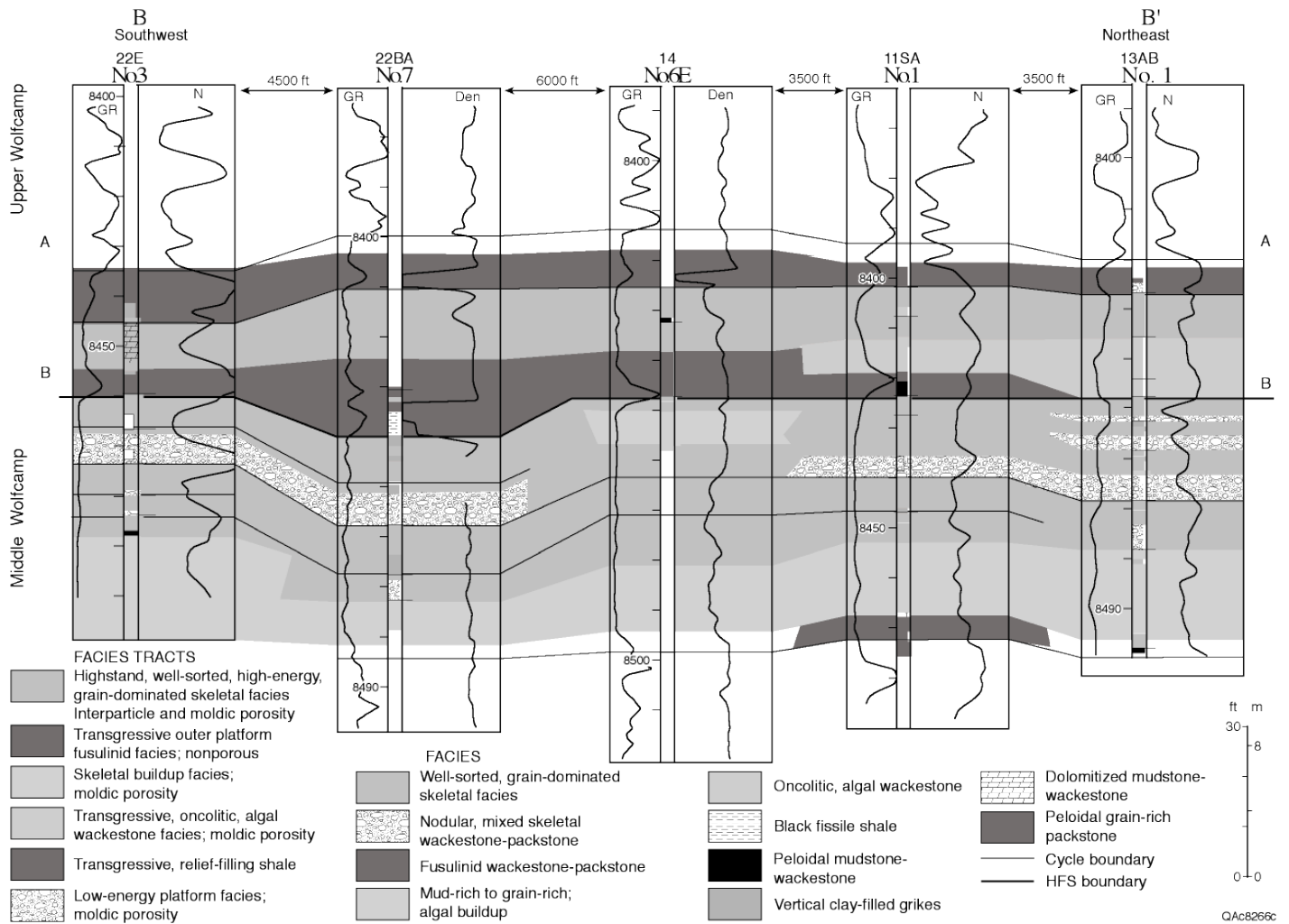


Figure 5. Cross section (B–B') depicting Wolfcamp stratigraphy, cyclicity, and facies distribution based on cored wells. Line of section shown in figure 2.

a.



b.

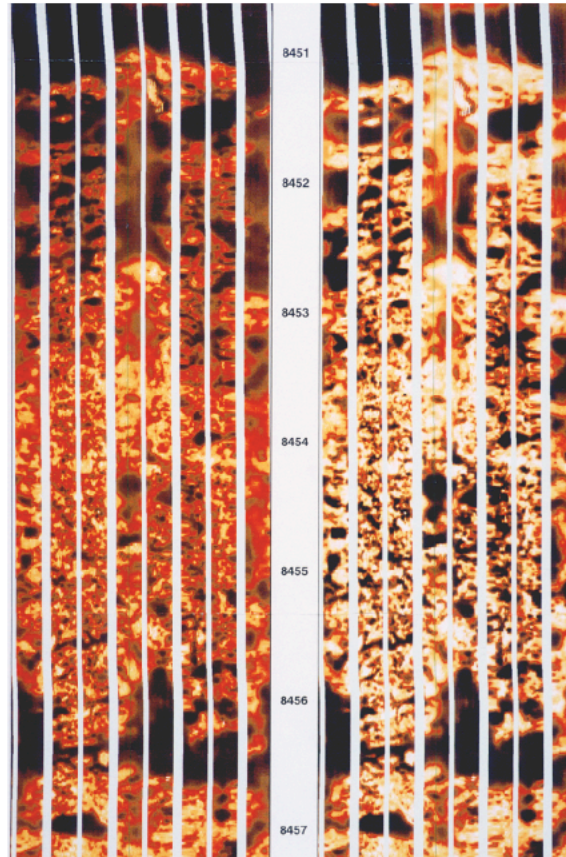


Figure 6. Paired photographs of skeletal wackestone/buildup facies from (a) core and (b) image log. Image log displays static image on left and dynamic image on right; depths are in feet. Cross Timbers 22 BA No. 7 well

a.



b.

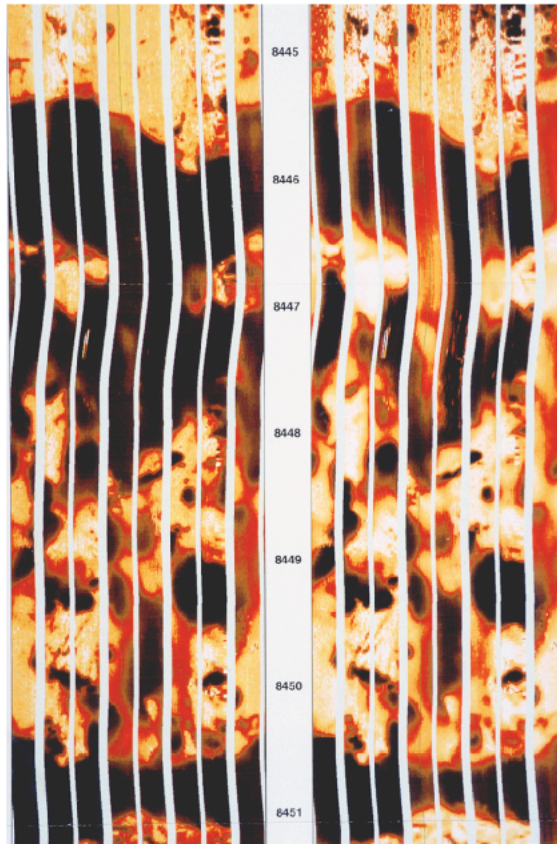


Figure 7. Paired photographs of karsted, cycle-top, peloid-skeletal packstone from (a) core and (b) image log. Vertical grikes are filled with greenish silt and clay. Although the image-log image is strongly dominated by the karst overprint, the granular appearance of the packstone is apparent. Image log displays static image on left and dynamic image on right; depths are in feet. Cross Timbers 22 BA No. 7 well.

a.



b.

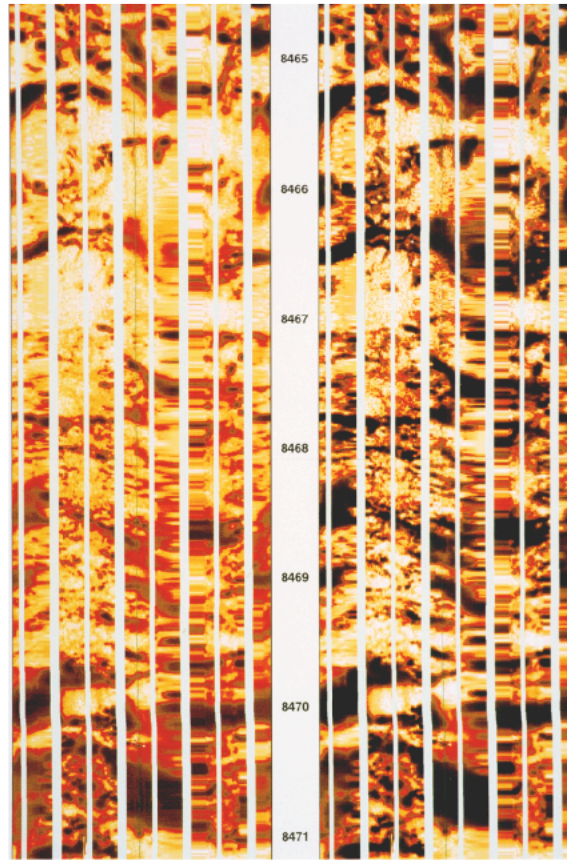


Figure 8. Paired photographs of stylolitic, nodular, skeletal wackestone from (a) core and (b) image log. Image log displays static image on left and dynamic image on right; depths are in feet. Cross Timbers 22 BA No. 7 well

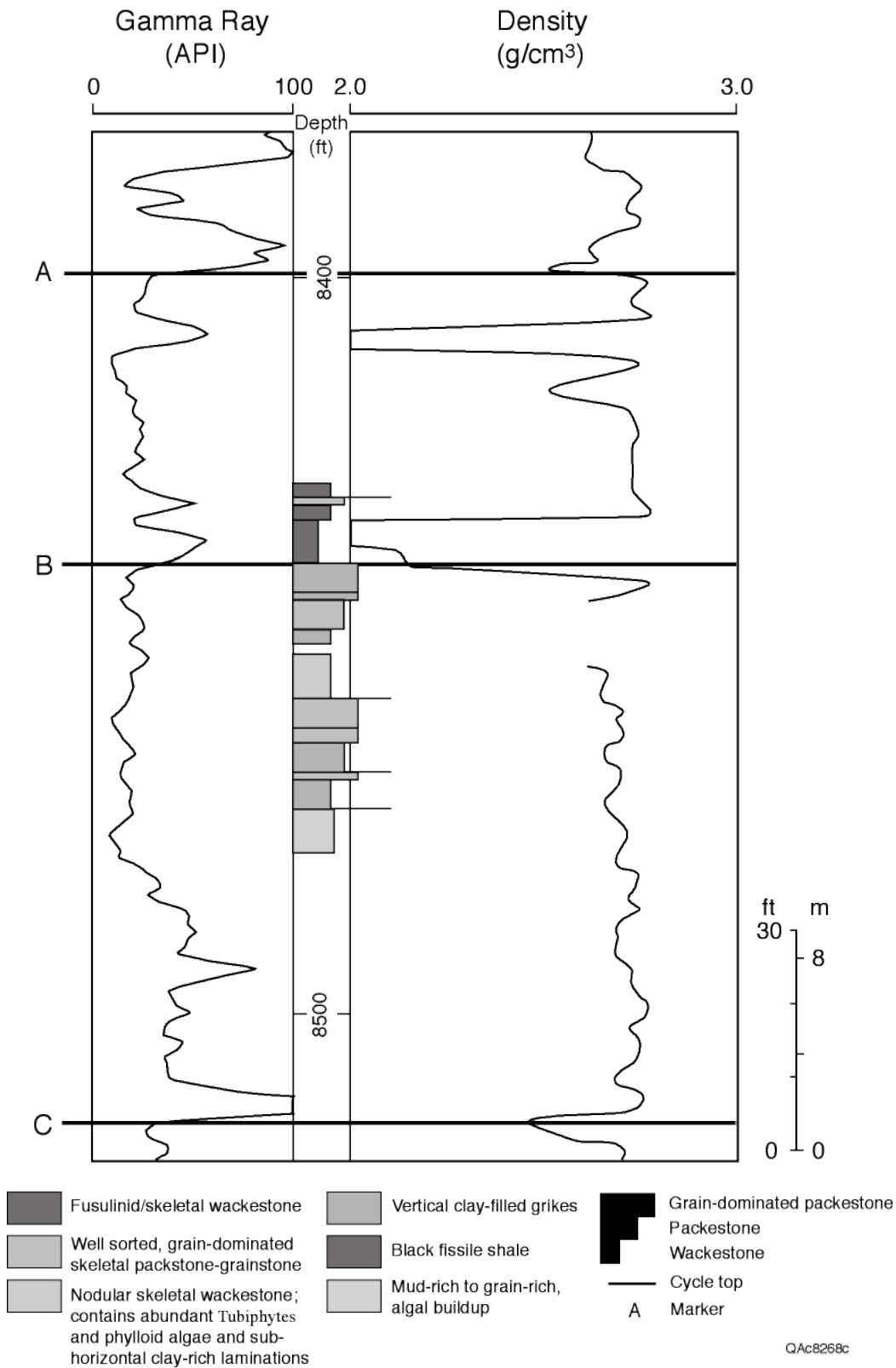


Figure 9. Wolfcamp facies succession and cyclicity based on core interpretation. Cross Timbers 22 BA No. 7 well.

a.



b.

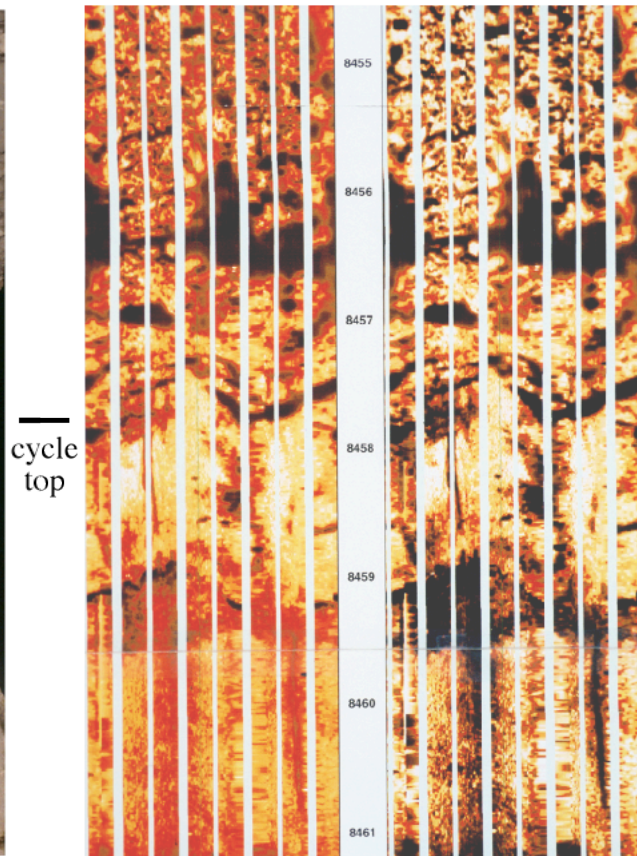
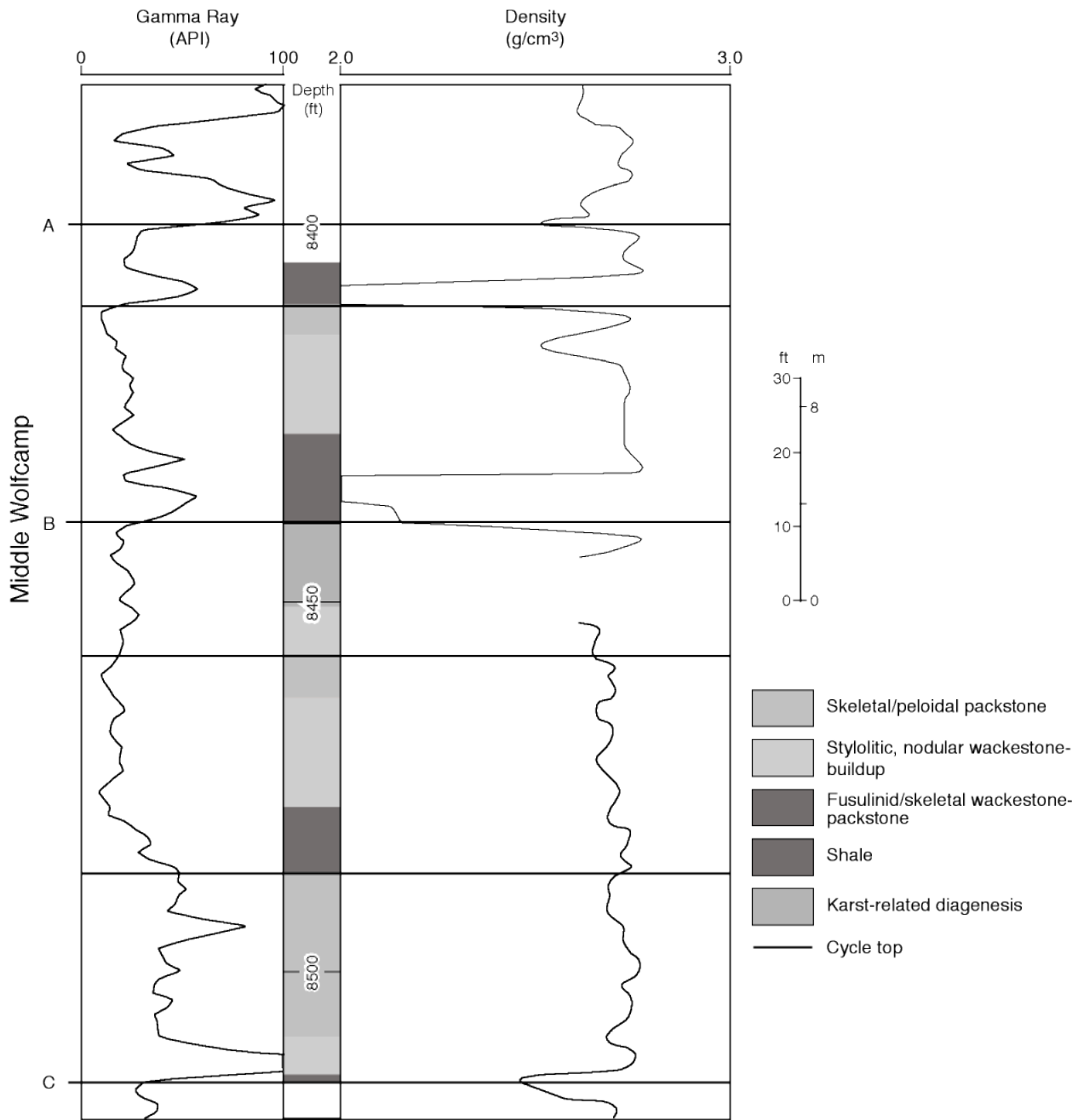


Figure 10. Paired photographs of (a) core and (b) image log showing cycle boundary with cycle-top, peloid-skeletal packstone and overlying cycle-base, nodular, skeletal wackestone. Note that dissolution pit at top of lower cycle is apparent on both core and image log. Image log displays static image on left and dynamic image on right; depths are in feet. Cross Timbers 22 BA No. 7 well.



QAc8269c

Figure 11. Wolfcamp facies succession and cyclicity based on image-log interpretation. Cross Timbers 22 BA No. 7 well.

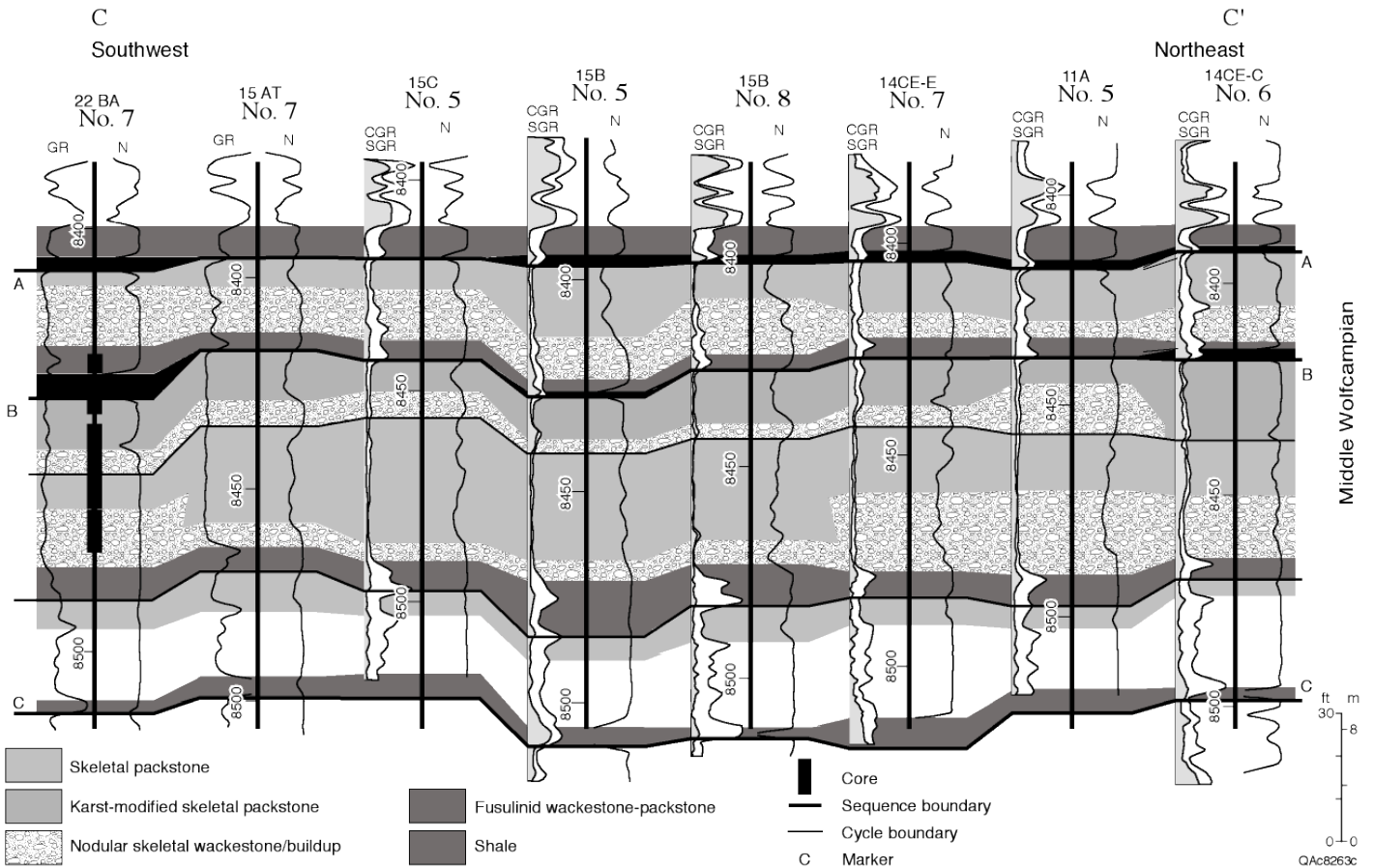


Figure 12. Cross section (C–C') depicting Wolfcamp stratigraphy, cyclicity, and facies distribution based on image logs. Line of section shown in figure 2.